

Electronic crossover in the normal state of $\text{YBa}_2\text{Cu}_4\text{O}_8$

A. Suter, M. Mali, J. Roos, and D. Brinkmann
Physik-Institut, Universität Zürich, CH-8057 Zürich, Switzerland

J. Karpinski and E. Kaldis
Laboratorium für Festkörperphysik, Eidgenössische Technische Hochschule Zürich, CH-8093 Zürich, Switzerland
 (Received 24 February 1997)

By performing nuclear magnetic resonance (NMR) and nuclear quadrupole resonance (NQR), respectively, with Cu, O, and Y isotopes in the normal state of the high-temperature superconductor $\text{YBa}_2\text{Cu}_4\text{O}_8$, we have found the following major results: (i) The Y, Cu, and O shift data support, for planes and chains, the validity of the “single-spin fluid model.” (ii) Around $T^* = 180$ K, “anomalies” in the temperature behavior of several NMR/NQR quantities have been detected. (iii) The anomalies do not arise from a structural phase transition; instead they reflect an electronic crossover which involves enhanced charge fluctuations in planes and chains accompanied by a charge (hole) transfer from chain to plane. (iv) As a possible mechanism of the crossover, a charge-density-wave instability is proposed. [S0163-1829(97)07533-4]

I. INTRODUCTION

The microscopic description of the electronic state, and in particular of the quasiparticles, of the normal conducting phase of high-temperature superconductors is still a matter of debate. It is commonly agreed that an understanding of the normal state is a prerequisite for the elucidation of the superconductivity mechanism. A typical question, not yet satisfactorily answered, concerns the origin of the spin pseudogap in underdoped cuprate superconductors. Thus, any additional information concerning the electronic state of the normal phase can be helpful.

In this paper, we will report on the detection of “anomalies” which are displayed in the temperature dependence of several nuclear magnetic resonance (NMR) and nuclear quadrupole resonance (NQR) quantities measured in the normal state of $\text{YBa}_2\text{Cu}_4\text{O}_8$. We will provide evidence that the anomalies do not arise from a structural phase transition, instead they are the fingerprint of an electronic crossover which involves an enhanced charge fluctuation in planes and chains accompanied by a charge (hole) transfer from chain to plane. As a possible mechanism of the crossover we will propose a charge-density-wave instability.

The paper is organized as follows. The next section will review the NMR-NQR background necessary to understand results and discussion. Section III will provide some information on the experimental techniques including the characterization of the sample. In Sec. IV we present and analyze our data, followed by a discussion in Sec. V and a summary in Sec. VI.

II. THEORY

A nuclear spin interacts with its electronic environment through electric and magnetic hyperfine couplings.¹ In the presence of an applied magnetic field \mathbf{B}_0 , the Hamiltonian of a nuclear spin \mathbf{I} having a quadrupole moment eQ can be written as

$$\mathcal{H} = \mathcal{H}_{\text{Zeeman}} + \mathcal{H}_{\text{quadrupole}} + \mathcal{H}_{\text{hyperfine}} \quad (1)$$

with

$$\mathcal{H}_{\text{Zeeman}} = -\gamma_n \hbar B_0 (I_z \cos \theta + I_y \sin \theta \sin \phi + I_x \sin \theta \cos \phi), \quad (2)$$

$$\mathcal{H}_{\text{quadrupole}} = \frac{eQV_{zz}}{4I(2I-1)} \left[3I_z^2 - \mathbf{I}^2 + \frac{\eta}{2}(I_+^2 + I_-^2) \right], \quad (3)$$

and

$$\mathcal{H}_{\text{hyperfine}} = \gamma_n \hbar \left(\sum_j \mathbf{I} \cdot \mathbf{A}_j \cdot \mathbf{S}_j + \mathbf{I} \cdot \mathbf{O} \cdot \mathbf{L} \right). \quad (4)$$

Here, $V_{\alpha\alpha}$ ($\alpha = x, y, z$) denote the principle components of the electric-field-gradient (EFG) tensor \mathbf{V} , with the axes labeled according to the convention $|V_{xx}| \leq |V_{yy}| \leq |V_{zz}|$. The asymmetry parameter of \mathbf{V} , η , is defined as $\eta = (V_{xx} - V_{yy})/V_{zz}$, $\eta \in [0, 1]$. For a particular site, x, y, z are chosen as the references in Eqs. (1)–(4). In all Y-Ba-Cu-O compounds, due to symmetry, one permutation of the x, y, z set coincides with the orthorhombic \mathbf{a}, \mathbf{b} , and \mathbf{c} crystal axes. θ and ϕ are the polar and azimuth angles, respectively, of \mathbf{B}_0 in this crystal frame. \mathbf{S}_j is the electron-spin operator at the copper site j and \mathbf{A}_j is its spin hyperfine tensor, the sum over j includes only on-site copper and its first neighbors. \mathbf{L} is the electron orbital angular momentum and \mathbf{O} is its on-site orbital hyperfine tensor. γ_n is the nuclear gyromagnetic ratio.

In our NMR experiments, B_0 is large and hence $\mathcal{H}_{\text{quadrupole}} \ll \mathcal{H}_{\text{Zeeman}}$. As a result, for each isotope and each site, the NMR signal is split into a central line arising from the central transition, $(+\frac{1}{2}, -\frac{1}{2})$, and into satellite lines. The $^{63,65}\text{Cu}$ nuclei ($I = 3/2$) produce two satellites arising from the $(\pm\frac{1}{2}, \pm\frac{3}{2})$ transitions, while the ^{17}O signal ($I = 5/2$) con-

tains, in addition, two outer satellites due to the $(\pm \frac{3}{2}, \pm \frac{5}{2})$ transitions. For ^{89}Y ($I=1/2$), there is no quadrupole splitting because for spin-half nuclei $eQ=0$. Finally, the $\mathcal{H}_{\text{hyperfine}}$ term causes a magnetic shift of each line.

If we set $B_0 = 0$, $\mathcal{H}_{\text{quadrupole}}$ gives rise to doubly degenerate energy levels between which NQR transitions can be induced. For the $^{63,65}\text{Cu}$ nuclei, a single NQR signal at frequency

$${}^{63,65}\nu_Q = \frac{e^{63,65}QV_{zz}}{2h} \sqrt{1 + \frac{1}{3}\eta^2} \quad (5)$$

is observed.

In the NMR experiments, the *magnetic* coupling between the nuclear spin and its electronic environment as expressed by the $\mathcal{H}_{\text{hyperfine}}$ Hamiltonian, (4) can be viewed as a coupling of the nuclear spin with a time-dependent local magnetic hyperfine field \mathbf{H}_L , generated by the electron spin and the electron orbital motion. The static part of \mathbf{H}_L gives rise to a NMR line shift expressed by the *magnetic shift tensor* \mathbf{K} , whose components, in the x, y, z reference frame, can be decomposed in a spin and an orbital part:

$$K_{\alpha\alpha}(T) = K_{\alpha\alpha}^{\text{spin}}(T) + K_{\alpha\alpha}^{\text{orbit}}. \quad (6)$$

The spin part of the magnetic shift is usually called the Knight shift. In the high- T_c compounds, $\mathbf{K}^{\text{orbit}}$ is predominantly temperature independent, whereas the temperature-dependent \mathbf{K}^{spin} is expected to vanish in the superconducting state due to singlet spin pairing.

Each part of the \mathbf{K} tensor can be expressed by the respective hyperfine interaction tensor and the static electronic susceptibility as

$$K_{\alpha\alpha}^{\text{spin}} = \frac{1}{g\mu_B} \sum_j (A_j)_{\alpha\alpha} (\chi_j)_{\alpha\alpha}, \quad (7)$$

$$K_{\alpha\alpha}^{\text{orbit}} = \frac{1}{\mu_B} O_{\alpha\alpha} \chi_{\alpha\alpha}^{\text{orbit}}. \quad (8)$$

The fluctuating part of \mathbf{H}_L is the source of the nuclear-spin-lattice relaxation. In the case of high- T_c compounds, the main contribution to the copper, oxygen and yttrium spin-lattice relaxation stems from the electron-spin fluctuations. After Moriya,² this contribution is related to the imaginary part of the dynamical spin susceptibility, $\chi(\mathbf{q}, \omega_0)$, and the ‘‘relaxation rate per temperature unit,’’ $(T_1 T)^{-1}$, is given by

$$\left(\frac{1}{T_1 T} \right)_{\alpha} = \frac{\gamma_n^2 k_B}{2\mu_B^2} \sum_{\mathbf{q}, \alpha' \neq \alpha} F_{\alpha'\alpha}(\mathbf{q}) \frac{\chi''_{\alpha'\alpha'}(\mathbf{q}, \omega_0)}{\omega_0}, \quad (9)$$

where

$$F_{\alpha}(\mathbf{q}) = \left| \sum_j A_{j,\alpha} \exp(i\mathbf{q} \cdot \mathbf{r}_j) \right|^2.$$

Here, ω_0 is the nuclear resonance frequency, α denotes the direction of quantization, i.e., the direction of V_{zz} in NQR and of B_0 in NMR experiments, and α' is the direction perpendicular to α . A_j is the on-site ($\mathbf{r}_j = \mathbf{0}$) and transferred ($\mathbf{r}_j \neq \mathbf{0}$) hyperfine coupling tensor for the nuclei under consideration. Thus, $(T_1 T)^{-1}$ provides information about the \mathbf{q}

averaged imaginary part of $\chi(\mathbf{q}, \omega_0)$. For convenience, we quite often will use the abbreviation $2W = 1/T_1$.

In case that there would also be fluctuating field gradients at the Larmor frequency, ω_0 , additional terms would appear in Eq. (9).³ These terms are usually negligible in high-temperature superconductors.

For the particular case where the hyperfine Hamiltonian (4) is approximated by the Mila-Rice Hamiltonian,⁴ the form factors $F_{\alpha}(\mathbf{q})$ for the different sites are given by^{4,5}

$${}^{63}F_{ab,c}(\mathbf{q}) = \{A_{ab,c} + 2B[\cos(q_x a) + \cos(q_y b)]\}^2, \quad (10)$$

$${}^{17}F_{\alpha}(\mathbf{q}) = \cos^2(q_x a/2) [C_{\alpha\alpha} + 2C'_{\alpha\alpha} \cos(q_y b)]^2 + \cos^2(q_y b/2) [C_{\alpha\alpha} + 2C'_{\alpha\alpha} \cos(q_x a)]^2, \quad (11)$$

$${}^{89}F_{\alpha}(\mathbf{q}) = \left[8D_{\alpha\alpha} \cos\left(\frac{q_x a}{2}\right) \cos\left(\frac{q_y b}{2}\right) \cos\left(\frac{q_z c'}{2}\right) \right]^2. \quad (12)$$

Here, $A_{ab,c}$ is the direct on-site coupling of the $^{63,65}\text{Cu}$ nuclei to the Cu^{2+} spin and B is the strength of the transferred hyperfine coupling of the $^{63,65}\text{Cu}$ nuclear spin to the four nearest-neighbor Cu^{2+} spins. $C_{\alpha\alpha}$ and $C'_{\alpha\alpha}$ are the transferred hyperfine coupling of the ^{17}O nuclear spin to its nearest- and next-nearest neighbor Cu^{2+} spins, respectively. The $C'_{\alpha\alpha}$ term was not included in the original Mila-Rice Hamiltonian.⁴ Finally, $D_{\alpha\alpha}$ is the coupling of the ^{89}Y nuclear spin to its nearest-neighbor Cu^{2+} spins and c' denotes the distance between nearest CuO_2 planes.

In the phenomenological Millis-Monien-Pines model,⁶ one includes, in addition to the normal Fermi-liquid contribution to the spin-lattice relaxation, strong antiferromagnetic fluctuations which lead to the anomalous behavior of the spin-lattice relaxation in high-temperature superconductors. In this model $\chi''(\mathbf{q}, \omega)$ is given by

$$\lim_{\omega \rightarrow 0} \chi''(\mathbf{q}, \omega) = \frac{\pi \chi_0 \hbar \omega}{\Gamma} \left[1 + \beta \frac{\xi^4}{[1 + (\mathbf{q} - \mathbf{Q}_{\text{AF}})^2 \xi^2]^2} \right] \quad (13)$$

or

$$\lim_{\omega \rightarrow 0} \chi''(\mathbf{q}, \omega) = \frac{\pi \chi_0 \hbar \omega}{\Gamma} [1 + \beta \xi^4 \exp(-(\mathbf{q} - \mathbf{Q}_{\text{AF}})^2 \xi^2)], \quad (14)$$

where ξ is the slightly temperature-dependent correlation length of the antiferromagnetic fluctuations and β is a measure for the relative strength of these fluctuations. χ_0 is defined as the static uniform spin susceptibility, Γ is an energy scale, and \mathbf{Q}_{AF} is the antiferromagnetic wave vector.

III. EXPERIMENTAL

The $\text{YBa}_2\text{Cu}_4\text{O}_8$ samples investigated in this work were prepared by the solid-state reaction technique which is described in detail elsewhere.⁷ One sample is the same one we used in previous $^{63,65}\text{Cu}$ and ^{17}O NMR/NQR experiments.^{8,9}

For oxygen NMR experiments, only ^{17}O , which possesses a nuclear spin, is suitable. Since the ^{17}O abundance is only

0.037%, it is necessary to prepare ^{17}O -enriched samples.

The ceramic pellets of $\text{YBa}_2\text{Cu}_4\text{O}_8$ were synthesized from a mixture of prereacted $\text{YBa}_2\text{Cu}_3\text{O}_7$ and CuO under an O_2 pressure of 400 bars. After a reaction time of 20 h at a temperature of 1040 °C, the $\text{YBa}_2\text{Cu}_4\text{O}_8$ material was cooled down to room temperature at a cooling rate of 2 °C/min. The sample was then charged into an Al_2O_3 crucible and subsequently placed in a quartz-pyrex reaction chamber to which the ^{17}O container was connected. After evacuation of the whole setup to a pressure of 10^{-3} mbar, the break seal was fractured and ^{17}O gas was allowed to enter the reaction chamber where a pressure of nearly 1 bar was reached. The ^{17}O annealing took place at a temperature of 810 °C for 500 h.

X-ray-diffraction measurements detected the presence of small amounts of CuO and high-pressure Ba-cuprate as impurity phases. dc magnetization experiments at 14 Oe showed a clear decrease of the susceptibility at 81 K and a Meissner fraction of 36%.

In order to study the anisotropic properties of the $\text{YBa}_2\text{Cu}_4\text{O}_8$ compound, the Cu and O NMR experiments were carried out on a c -axis-oriented powder. The magnetic orienting of the powder, described in Ref. 10, produced a sample with a high degree of c -axis alignment of the grains whereas a and b axes remained randomly distributed.

The NQR and NMR experiments were performed by using standard pulse spectrometers. The NMR data were taken in a field of 8.9945 T. The resonance signals were obtained by a phase alternating add-subtract spin echo technique similar to that one described in Ref. 11. The spectra were obtained by Fourier transformation of the spin-echo. In all our experiments, we used very intense radio frequency pulses with optimal $\pi/2$ -pulse lengths of 1.6 μs or less, except for ^{89}Y NMR where the pulse length was ≈ 12 μs .

The nuclear-spin-lattice relaxation rate, $(1/T_1)_\alpha$, of ^{89}Y was measured by recording the spin-echo intensity after seven saturation pulses. In order to improve the signal-to-noise ratio, the Carr-Purcell-Meiboom-Gill pulse sequence¹² was applied with an accumulation of up to 16 spin-echo signals.

$(1/T_1)_\alpha$ of the plane oxygen, O(2,3), was measured by the inversion recovery sequence. In case of $(1/T_1)_c$, the magnetization recovery was measured on the first upper satellite. For $\mathbf{B} \perp \mathbf{c}$ measurements, however, the powder pattern produced by the random alignment in the ab plane creates a complication which was evaded by using a method proposed by Martindale *et al.*^{13,14}

For the chain oxygen, O(4), $(1/T_1)_c$ was obtained in the following way. Using an Ohmic-damped resonance circuit, we saturated simultaneously all the ^{17}O (4) lines which have a maximum separation of about 230 kHz. Given this initial condition, the recovery of the magnetization follows a single exponential and it is obtained by integrating the individual lines after Fourier transformation. In order to check whether we really saturated all the lines, we also analyzed each line by itself, which yielded the same $(1/T_1)_c$.

The NQR copper experiments were performed using an Ohmic-damped resonant circuit in order to ensure that we irradiated the whole line. The spectra were obtained by Fourier transformation of the spin echo. $1/T_1^{\text{NQR}}$ for the chain

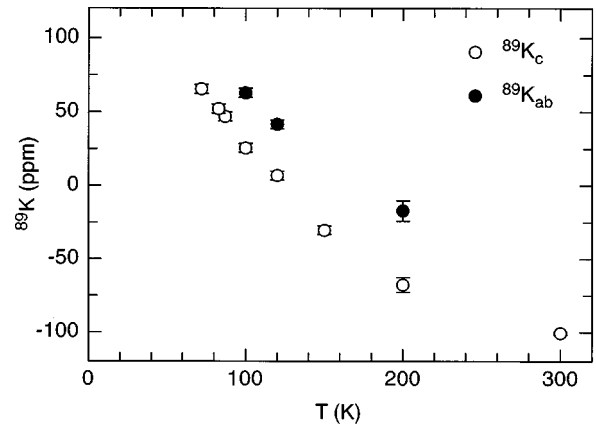


FIG. 1. ^{89}Y frequency shift in $\text{YBa}_2\text{Cu}_4\text{O}_8$. $^{89}\text{K}_{c,ab}$ shift for $c \parallel B_0$ ($^{89}\text{K}_c$) and $c \perp B_0$ ($^{89}\text{K}_c$).

copper, ^{63}Cu (1), was measured by the inversion recovery sequence.

IV. RESULTS AND ANALYSIS

A. Yttrium

Figure 1 shows, for two different field directions, the temperature dependence of the yttrium frequency shift $^{89}\text{K}_\alpha$ relative to the resonance in a YCl_3 solution. The signals are fairly narrow, with symmetric line shape and of a typical width (full width at half height) of 1.2 kHz which is almost temperature independent. Our data agree with results reported by other authors.^{15,16}

Previously, we had measured, in the very same sample, the oxygen shift $^{17}\text{K}_\alpha$ at the plane oxygen site O(2,3) and the copper shift $^{65}\text{K}_\alpha$ at the plane copper site Cu(2). The oxygen data have been supplemented by additional measurements. As shown in Fig. 2, the Cu and O shifts depend linearly on $^{89}\text{K}_c$ which implies the same temperature dependence. Hence, because of Eq. (6), $^{89}\text{K}^{\text{spin}}$ is linearly related to $^{17}\text{K}^{\text{spin}}$ and $^{65}\text{K}^{\text{spin}}$, respectively.

Taking the oxygen and copper orbital contributions from our previous analyses of the same sample,^{8,9} $^{17}\text{K}_c^{\text{orb}} = -0.007 \pm 0.01\%$ and $^{65}\text{K}_{ab}^{\text{orb}} = 0.28 \pm 0.02\%$, we calculated the yttrium orbital shifts as $^{89}\text{K}_c^{\text{orb}} = 170 \pm 15$ ppm

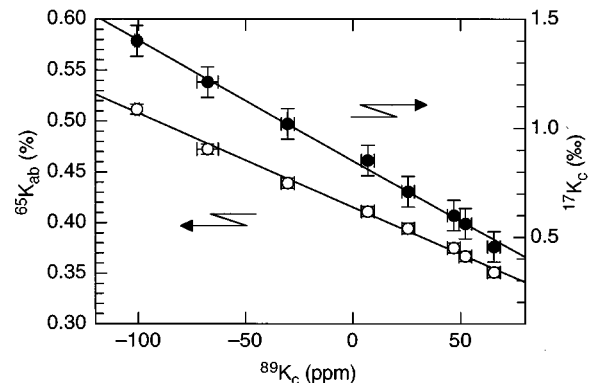


FIG. 2. ^{89}Y frequency shift plotted against ^{17}O (2,3) shift and ^{65}Cu (2) shift, respectively. ^{17}O (2,3) data are from Ref. 8 ^{65}Cu (2) data from Ref. 9.

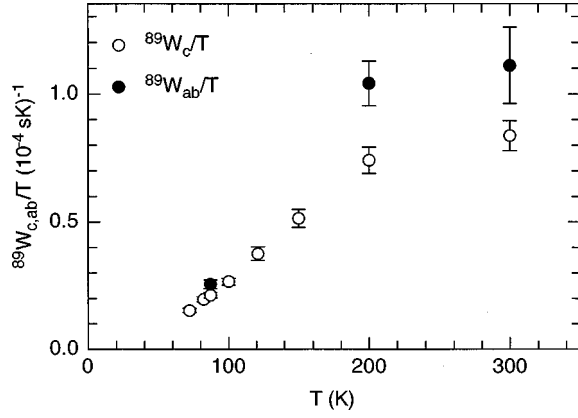


FIG. 3. Temperature dependence of $^{89}W_{c,ab}/T$ for field directions $c\parallel B_0$ ($^{89}W_c/T$) and $c\perp B_0$ ($^{89}W_{ab}/T$).

and $^{89}K_{ab}^{\text{orb}} = 175 \pm 15$ ppm, which agree with results of other authors.^{15–18} In this way we obtained the temperature dependence of $^{89}K_c^{\text{spin}}$.

The temperature dependence of the ^{89}Y spin-lattice relaxation rate per temperature unit, $^{89}W_\alpha/T$, is shown in Fig. 3 for two different field directions. We notice a rate anisotropy, defined as $^{89}(W_{ab}/W_c)$, which is temperature independent. Its value, 1.35 ± 0.1 , coincides almost with the square of the anisotropy of the hyperfine coupling constant, $(D_c^2 + D_{ab}^2)/(2D_{ab}^2) = 1.19$ (Ref. 15).

If the so-called Korringa relation would hold for yttrium, one would expect that $T_1 T (K^{\text{spin}})^2 = \kappa (\hbar/4\pi k_B) (\gamma_e/\gamma_n)^2$, where $\kappa = 1$ for the free-electron model and $(\hbar/4\pi k_B) (\gamma_e/\gamma_n)^2 = 1.1 \times 10^{-4}$ (K s) for ^{89}Y . Figure 4 shows, for the yttrium site, the temperature dependence of both $[T_1 T K^{\text{spin}}]_c$ and $[T_1 T (K^{\text{spin}})^2]_c$. Obviously, only the $[T_1 T (K^{\text{spin}})^2]_c$ data are nearly temperature independent thus demonstrating an almost Korringa-like behavior for the yttrium site with $\kappa \approx 3.5$.

A further check whether the Korringa relation holds, without knowing the orbital shift, is provided by the inset of Fig. 4 where we have plotted $(T_1 T)^{-1}$ and $(T_1 T)^{-1/2}$ versus the measured total magnetic shift K_c . Although both plots reveal a linear relationship, it is *only* the $(T_1 T)^{-1/2}$ plot that yields, when extrapolated to zero temperature, that is for $(T_1 T)^{-1/2} = 0$, an orbital shift which agrees, within experi-

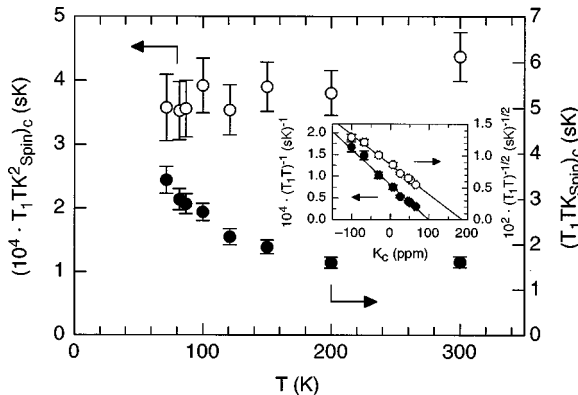


FIG. 4. Temperature dependence of $[T_1 T K^{\text{spin}}]_c$ and $[T_1 T (K^{\text{spin}})^2]_c$ at the yttrium site. In the inset, $(T_1 T)^{-1}$ and $(T_1 T)^{-1/2}$ are plotted against the measured total magnetic shift K_c .

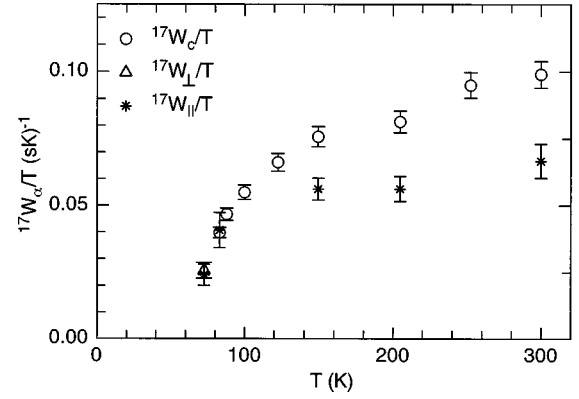


FIG. 5. Temperature dependence of $^{17}W_{c,\parallel,\perp}/T$ at O(2,3) site for field directions $c\parallel B_0$ ($^{17}W_c/T$) and $c\perp B_0$ ($^{17}W_{\perp,\parallel}/T$).

mental errors, with the value 170 ± 15 ppm we calculated above. Our result that the Korringa relation holds quite well for the Y site contrasts with the statement of Dupree *et al.*¹⁶

B. Oxygen

1. Plane oxygen

Figure 5 shows the spin-lattice relaxation rate per temperature unit of the plane oxygen nuclei O(2,3) for three orientations of the magnetic field. $^{17}W_c/T$ (with $B_0\parallel c$) was measured at the first satellite on the high-frequency side of the spectrum [the $(-3/2, -1/2)$ transition] to ensure that only signals of the O(2,3) sites were detected. $^{17}W_{\parallel}/T$ and $^{17}W_{\perp}/T$ refer to rates measured with the magnetic field perpendicular to c and either parallel or perpendicular to the Cu(2)-O bond axis. These rates were obtained by a method proposed by Martindale *et al.*^{13,14} using either the $(-5/2, -3/2)$ or $(3/2, 5/2)$ transition. Because the signals of the O(2,3) (Ref. 8) site and of the chain oxygen site, O(4) (Ref. 9), overlap around 110 K, there is a temperature region from 90 to 130 K where we cannot resolve clearly the edge in the spectra to extract $W_{\perp,\parallel}/T$.

Our present values for $^{17}W_c/T$ are slightly smaller than our previously published data¹⁹ because of the increased precision of the measurements due to a higher magnetic field which allowed us to monitor the magnetization recovery over a larger time interval. At temperatures above 160 K, these data are about 30% lower. Our present data are consistent with those measured by Zheng *et al.*,²⁰ but are, at temperatures above 160 K, lower than those of Tomeno *et al.*²¹ by about 30%.

Clearly, $^{17}W_c/T$ and $^{17}W_{\parallel}/T$ exhibit a remarkably different temperature behavior. To emphasize this fact, we plot, in Fig. 6, the ratio $^{17}(W_{\parallel}/W_{c,\perp})$ as a function of temperature. The point at the lowest temperature belongs already to the superconducting state. The solid line in Fig. 6 will be discussed in Sec. V.

2. Chain oxygen

The temperature dependence of $^{17}W_\alpha/T$ for the chain oxygen site O(4) is given in Fig. 7. Two plateaus are observed separated by a “kink” at approximately 200 K. The

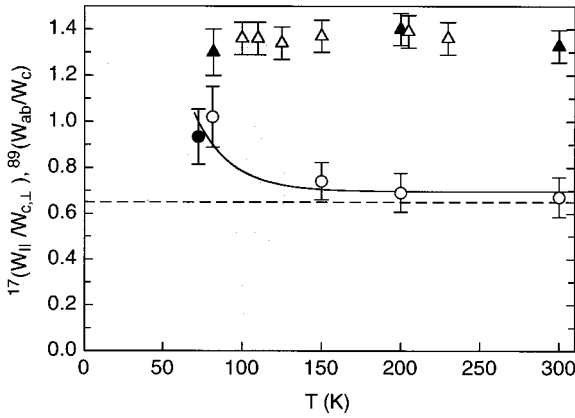


FIG. 6. Temperature dependence of $^{17}(W_{\parallel}/W_{c,\perp})$ and $^{89}(W_{ab}/W_c)$ for O(2,3) and Y, respectively. Open circles: $^{17}(W_{\parallel}/W_{c,\perp})$; bullet: $^{17}(W_{\parallel}/W_{\perp})$; open and black triangles: $^{89}(W_{ab}/W_c)$ (black triangles taken from Ref. 15). The dashed line is the value according to the Mila-Rice Hamiltonian (data for the hyperfine coupling constants from Ref. 15). The solid line is a fit according to Ref. 5. The shaded area is the temperature region, where we cannot extract $^{17}W_{\parallel,\perp}$.

presence of the kink is a clear sign for either a structural phase transition or a change in the electronic structure around 200 K.

The analysis of the spectra also yields the parameter of the EFG: $\eta=0.861(2)$ and $\nu_{zz}=eQV_{zz}/h=-411(5)$ kHz, which are essentially temperature independent in agreement with Mangelschots *et al.*⁸

C. Copper

1. Plane copper

For the plane copper site Cu(2), we have measured the temperature dependence of the following parameters: the frequency, $^{63}\nu_Q$, and the linewidth, $^{63}\delta\nu_Q$, of the ^{63}Cu NQR signal (Fig. 8, for comparison we also show $^{63}\delta\nu_Q$ of chain copper) and the total magnetic shift, $^{65}K_c$, and the corresponding linewidth, $^{65}\delta B$, of the ^{65}Cu NMR signal (Fig. 9).

Since the NQR line is almost symmetric we have defined $^{63}\nu_Q$ as the center of gravity of the top half of the line. The

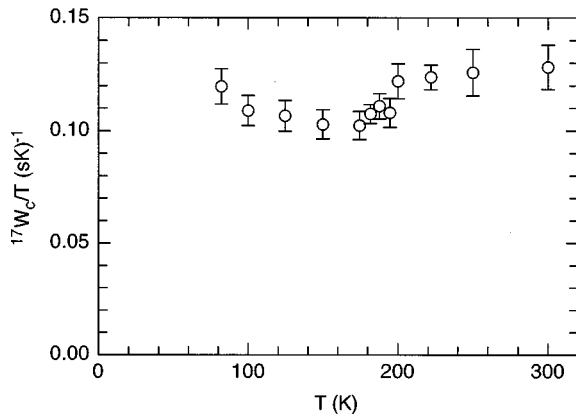


FIG. 7. Temperature dependence of $^{17}W_c/T$ for chain oxygen O(4) ($c\parallel B_0$).

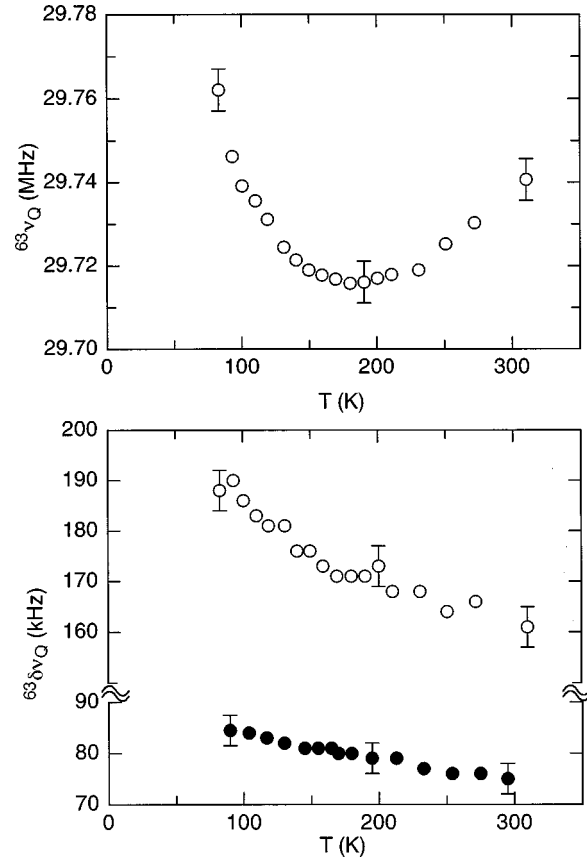


FIG. 8. Upper plot: NQR frequency $^{63}\nu_Q$ vs temperature of Cu(2). Lower plot: Corresponding quadrupolar linewidth $\delta\nu_Q$ (open circles) and $\delta\nu_Q$ of chain copper Cu(1) (bullets) vs temperature, respectively.

signal is *inhomogeneously* broadened due to quadrupolar interactions (Ref. 11). $^{63}\nu_Q$ shows a clear minimum, which was already observed by Zimmermann *et al.*,²² at about 180 K. At the same temperature, the temperature dependence of $^{63}\delta\nu_Q$ changes its slope.

The $^{65}\text{Cu}(2)$ NMR signal is very narrow and slightly asymmetric. Since $^{65}K_c$ is huge, we defined $^{65}K_c$ as the center of gravity of the upper 30% of the signal. Thus, we could measure $^{65}K_c$ within an accuracy of 0.002%. Again, around 180 K, we notice anomalies in both $^{65}K_c$ and $^{65}\delta B$. Below this temperature, the shifts start to increase and the temperature dependence of $^{65}\delta B$ changes its slope.

2. Chain copper

For the NQR signal of the chain copper site Cu(1), we have measured the temperature dependence of the NQR frequency, $^{63}\nu_Q$ (Fig. 10), and the NQR spin-lattice relaxation rate, $^{63}(1/T_1^{\text{NQR}})$ (Fig. 11). Since the NQR line is almost symmetric we determined $^{63}\nu_Q$ in the same way as for the plane copper.

Although $^{63}\nu_Q$ does not exhibit a minimum as found for Cu(2), there is again, at 180 K, a clear change in the slope of the temperature dependence of $^{63}\nu_Q$. The corresponding linewidth, $^{63}\delta\nu_Q$ is shown in Fig. 8 and shows within the resolution no effect at 180 K. However, also the $^{63}(1/T_1^{\text{NQR}})$ data reveal a slight but distinct change of the slope at the same temperature.

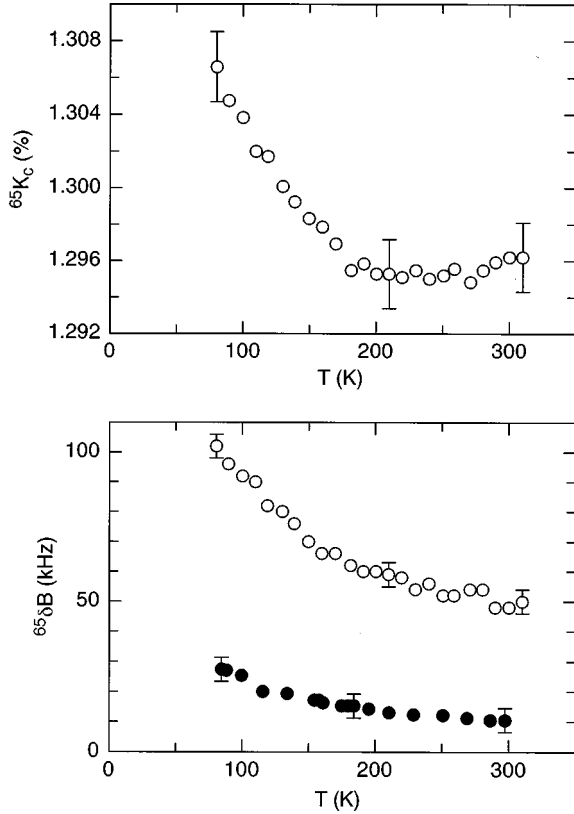


FIG. 9. Upper plot: Temperature dependence of the total magnetic shift $^{65}K_c$ for plane copper Cu(2), $c \parallel B_0$. Lower plot: Corresponding magnetic linewidth δB (open circles) and δB of chain copper, Cu(1) (bullets, Ref. 9) vs temperature, respectively.

V. DISCUSSION

Based on our results, we will now discuss three major topics, the single-spin fluid model, the anomalies around 180 K, and the anisotropy of the plane oxygen and yttrium relaxation rates.

A. Single-spin fluid model

The additional measurements of the Y magnetic shift supplement our previous Cu and O shift studies,⁹ where we have shown that the various shift components exhibit the same temperature dependences over a large temperature

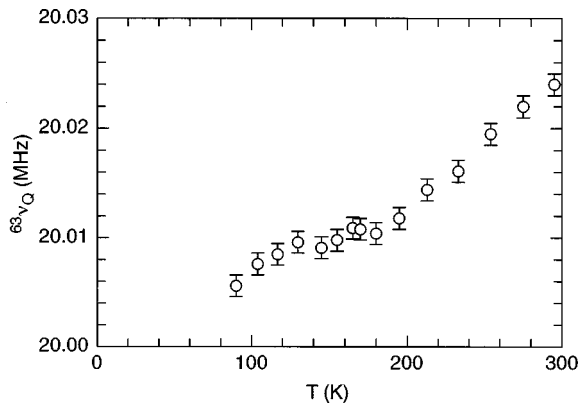


FIG. 10. Temperature dependence of the chain copper Cu(1) NQR frequency $^{63}\nu_Q$.

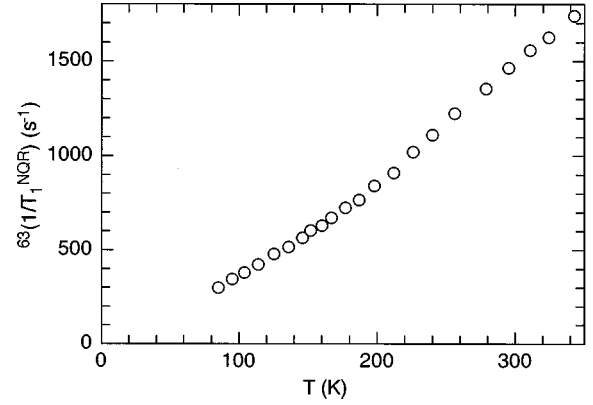


FIG. 11. Temperature dependence of $^{63}(1/T_1^{\text{NQR}})_c$ of chain copper Cu(1).

range (see Fig. 2). These facts support the “single-spin fluid model” which states that the Cu 3d holes and the doped holes, which mainly go into O 2p states,^{4,23} have one spin degree of freedom. The same scaling is also found for the magnetic shifts of O(4) and Cu(1) of the double chain.⁹ However, the susceptibilities of the two systems are different.

B. Anomalies around 180 K

We summarize the NMR/NQR parameters for which we have detected an anomalous behavior in their temperature dependences around $T^\dagger = 180$ K: (i) Plane copper Cu(2): frequency $^{63}\nu_Q$ and linewidth $^{63}\delta\nu_Q$ of the NQR signal, total magnetic shift $^{65}K_c$ and linewidth $^{65}\delta B$ of the NMR signal; (ii) Chain copper Cu(1): frequency and spin-lattice relaxation rate of the NQR signal; (iii) Chain oxygen O(4): spin-lattice relaxation rate of the NMR signal; and (iv) ratio of the yttrium and plane oxygen spin-lattice relaxation rates.

The first question to be answered is whether these facts reflect the presence of a structural phase transition or a change in the electronic structure only. The occurrence of a *first-order* phase transition can be ruled out for the following reason. Since ν_Q is proportional to V_{zz} [see Eq. (5)], it is a quantity which is very sensitive to structural changes and ν_Q would alter its value remarkably at the temperature where the transition takes place. However, neither $^{63}\nu_Q$ of Cu(1) (Fig. 10) nor $^{63}\nu_Q$ of Cu(2) (Fig. 8) show a “jump” at T^\dagger . $^{63}\nu_Q$ of Cu(1) merely exhibits a change in slope and $^{63}\nu_Q$ of Cu(2) passes through a broad minimum around T^\dagger . Although these changes would be compatible with a second-order structural phase transition, we also can rule out such a transition on the following grounds. In a previous study,²⁴ we obtained a perfectly “smooth” temperature dependence of ν_Q of ^{137}Ba from 17 up to 400 K and the linewidth remains constant in that range. We did not detect any anomaly, neither in the frequency nor in the width of the Ba signal. Furthermore, x-ray studies,^{25–27} revealed no anomalies around T^\dagger in pure $\text{YBa}_2\text{Cu}_4\text{O}_8$,²⁸ and ultrasonic attenuation studies²⁹ did not find an enhancement of the attenuation coefficient at T^\dagger . We thus conclude that the anomalies occurring at T^\dagger do not arise from a structural phase transition but are the signature of a change or a crossover in the electronic system that leaves the time-averaged spatial structure essentially untouched.

Based on these results, we conclude that the changes, at T^\dagger , of the two dynamic parameters $^{17}W_c/T$ of O(4) and $^{63}(1/T_1^{\text{NQR}})$ of Cu(1) can also be attributed to a change in the electronic system. While the temperature dependence of $^{63}(1/T_1^{\text{NQR}})$ of Cu(1) (Fig. 11) changes its slope, $^{17}W_c/T$ of O(4) displays a clear step with a plateau above as well as below T^\dagger (Fig. 7). Both phenomena are not compatible with a simple metallic behavior for which one would expect $T_1 T = \text{const}$.

We suggest that the electronic crossover results in an opening of an additional relaxation channel for spin-lattice relaxation of both Cu(1) and O(4) and that the mechanism of the additional relaxation is of quadrupolar origin due to charge fluctuations in the chain. In other words, the electronic crossover taking place at T^\dagger is *dynamic* on the NMR/NQR time scale which is of the order of 10^{-5} – 10^{-9} s. If the crossover would be static rather than dynamic, one would have observed, in addition to the change of $^{17}W_c/T$, a variation in the magnetic shift $^{17}K_c$, in contrast to our earlier measurements.⁹

The conclusion that the crossover is dynamic rather than static is supported by a pulsed-neutron-scattering experiment,³⁰ where the analysis of the pair-distribution function provided evidence for the formation of dynamic and electrically polarized microdomains in the chain for temperatures below T^\dagger . These domains are mainly caused by a spatial displacement, perpendicular to the chain, of chain oxygen. As Zhou *et al.*³¹ pointed out, the presence of these domains would explain, in a very natural way, resistivity data taken by these authors, namely the change in the temperature derivative of the resistivity along the a axis and the minimum in the derivative of the c axis resistivity.

Next, we address the question whether the crossover just described is restricted to the electronic system of the chains or whether the planes are also involved. As summarized above, several Cu(2) parameters exhibit anomalies around T^\dagger . We will start by discussing $^{63}\nu_Q$ and $^{63}\delta\nu_Q$ (Fig. 8) of the Cu NQR signal.

The field-gradient component V_{zz} , which appears in the expression for $^{63}\nu_Q$, is composed of a valence part V_{zz}^{val} and a lattice part V_{zz}^{lat} , which is negative since the main contribution arises from oxygen. Because the shrinking of the lattice, with falling temperature, determines the temperature dependence of V_{zz}^{lat} , this quantity becomes more negative if the temperature is lowered. On the other hand, V_{zz}^{val} is positive and is assumed to be temperature independent; furthermore, $|V_{zz}^{\text{val}}| > |V_{zz}^{\text{lat}}|$. Thus, one would expect $^{63}\nu_Q$ to decrease, with decreasing temperature, in a monotonic fashion, in contrast to the experimental facts.

In the framework of the present discussion, the appearance of the broad $^{63}\nu_Q$ minimum is difficult to understand. Zimmermann¹¹ tried to explain it in terms of an inhomogeneous shrinking of the lattice²⁵ that would produce different lattice contributions from O(2,3) and O(4), which also differ in sign. However, this assumption does not explain consistently the $^{63}\nu_Q$ temperature dependence for Cu(1). Therefore, we postulate, in addition to Zimmermann's assumption, a charge redistribution to occur below T^\dagger , namely a transfer of holes from the chains into the planes. Such a transfer, below T^\dagger , would increase V_{zz}^{val} and, hence, $^{63}\nu_Q$ of Cu(2).

Together with the broad $^{63}\nu_Q$ minimum, we notice an enhancement of the increase of the linewidth $\delta\nu_Q$. The line is inhomogeneously broadened²² due to quadrupolar interactions¹¹, i.e., there is a distribution of electric-field gradients. The enhancement of the broadening below T^\dagger indicates that the proposed charge redistribution is not completely homogeneous. It is important to note that the Cu(1) signal (see Fig. 8) is much narrower than the Cu(2) signal and does not get broader below T^\dagger . This seems to be evidence that the origin of the anomaly is located in the plane rather than in the chain.

Finally, we turn to the magnetic shift K_c of Cu(2). A very puzzling fact is that this quantity is almost temperature independent but has a huge value^{9,32–34} in the whole Y-Ba-Cu-O family and in $\text{La}_{2-x}\text{Sr}_x\text{CuO}_4$. In the literature, one has argued that the spin part of K_c vanishes since K_c does not change at the transition from the normal to the superconducting phase. In the framework of the Mila-Rice Hamiltonian, this means that $A_c + 4B = 0$.

Our measurements of $^{65}K_c$ (Fig. 9) demonstrate that the relation $A_c + 4B = 0$ is in agreement with experiment for temperatures larger than T^\dagger but is slightly violated below this temperature provided the orbital part of $^{65}K_c$ is still temperature independent. To explain the data below T^\dagger , we must require $A_c + 4B > 0$ which implies that either the positive¹⁵ B must have increased or the negative A_c has decreased. Such modifications of the hyperfine couplings cannot be traced back to changes of local atomic distances because the thermal shrinking shows no effect above T^\dagger . Instead, a slight increase of the amount of holes in the plane, which is a process consistent with our discussion of $^{63}\nu_Q$, explains the observations. That the tiny change of $^{65}K_c$ at T^\dagger has been detected at all, is based on the almost perfect cancellation of A_c and B . Therefore, no anomaly could be observed, for instance, in $^{65}K_{ab}$.

The anomaly of $^{65}K_c$ at T^\dagger is accompanied by a change of the temperature derivative of the linewidth, $^{65}\delta B$, of the NMR signal. The origin of the *inhomogeneous* broadening is of magnetic nature, i.e., due to a distribution of local magnetic fields. The width of the corresponding Cu(1) NMR signal is much smaller and also shows a slight change in slope at T^\dagger , although less pronounced than the change of the Cu(2) linewidth. This change of the Cu(1) NMR linewidth contrasts with the behavior of the Cu(1) NQR linewidth which does not exhibit an anomaly at T^\dagger .

C. Anisotropy of plane oxygen and yttrium relaxation

We will turn now to the effect of the inplane charge fluctuations on the plane copper, Cu(2), and oxygen, O(2,3). First, we will discuss the anisotropy of the O(2,3) spin-lattice relaxation rate, that is the ratio $^{17}(W_{\parallel}/W_c)$ (see Sec. IV B 1), and we will show that the standard Mila-Rice Hamiltonian fails to explain the temperature dependence of the anisotropy. Then, we will demonstrate that the proposal by Zha *et al.*⁵ does not provide a *consistent* description of the temperature dependences of both $^{17}(W_{\parallel}/W_c)$ and $^{17}W_c/^{89}W_c$. Based on these findings and the results of Sec. V B, we then propose the presence of *additional* charge fluctuations and, in this way, we achieve a coherent description of all the data.

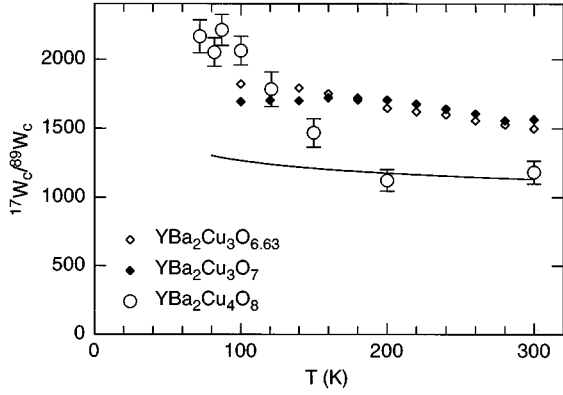


FIG. 12. $^{17}W_c/^{89}W_c$ vs temperature. Open circle, present work; open and black diamonds from Ref. 17. The solid line is a calculation following Ref. 5.

Figure 6 shows the temperature dependence of $^{89}(W_{ab}/W_c)$ and $^{17}(W_{\parallel}/W_{c,\perp})$.³⁵ $^{89}(W_{ab}/W_c)$ remains temperature independent, while $^{17}(W_{\parallel}/W_{c,\perp})$ displays a remarkably strong temperature dependence below T^\dagger . Similar temperature dependences of $^{17}(W_{\parallel}/W_{c,\perp})$, but much less pronounced, were found in $\text{YBa}_2\text{Cu}_3\text{O}_{6.5}$,³⁶ $\text{YBa}_2\text{Cu}_3\text{O}_{6.52}$,³⁷ and $\text{YBa}_2\text{Cu}_3\text{O}_{6.96}$,¹⁴ in the latter compound, which is optimally doped, the temperature dependence is weakest.

The temperature dependence of $^{17}(W_{\parallel}/W_{c,\perp})$ is difficult to understand in the framework of the Mila-Rice Hamiltonian which predicts $^{17}(W_{\parallel}/W_c) = (C_c^2 + C_\perp^2)/(C_c^2 + C_\perp^2)$. Since just hyperfine coupling constants C_α are involved,³⁸ $^{17}(W_{\parallel}/W_{c,\perp})$ should be temperature independent. Taking the C_α values given by Kambe *et al.*,¹⁵ one finds $^{17}(W_{\parallel}/W_{c,\perp}) \approx 0.65$, which describes the high-temperature values very well but fails at temperatures below T^\dagger .

Zha *et al.*⁵ tried to explain the behavior of $^{17}(W_{\parallel}/W_{c,\perp})$ in the framework of the Millis-Monien-Pines model⁶ by including additional next-nearest-neighbor coupling [see Sec. II and Eq. (11)] and incommensurate antiferromagnetic fluctuations with wave vector \mathbf{Q}_i . The authors found that

$$\frac{^{17}W_\alpha}{^{17}W_\beta} \approx \frac{S_\alpha}{S_\beta} \left[1 + \left(\frac{P_\alpha}{S_\alpha} - \frac{P_\beta}{S_\beta} \right) \left(\frac{1}{^{63}T_{1c} T \chi_0(T)} \right) \right], \quad (15)$$

where $\alpha, \beta = \parallel, \perp, c$, $P_{\alpha, \beta} = ^{17}F_{\alpha, \beta}(\mathbf{Q}_i) / ^{63}F_c(\mathbf{Q}_i)$ and

$$S_{\alpha, \beta} \approx \frac{\pi}{\Gamma} \int_{\text{BZ}} ^{17}F_{\alpha, \beta}(\mathbf{q}) d^2q. \quad (16)$$

The crucial point of this approach is that incommensurate antiferromagnetic fluctuations are invoked whose existence, in the Y-Ba-Cu-O family, is still unclear. For instance, neutron-scattering experiments in $\text{YBa}_2\text{Cu}_3\text{O}_7$ (Refs. 39,40,42), $\text{YBa}_2\text{Cu}_3\text{O}_{6.63}$ (Refs. 43,44), and $\text{YBa}_2\text{Cu}_3\text{O}_{6.60}$ (Ref. 41) just show comparatively broad temperature-independent peaks for \mathbf{Q}_{AF} .

Nevertheless, as shown in Fig. 6, Eq. (15) is able to describe the temperature dependence of $^{17}(W_{\parallel}/W_{c,\perp})$ quite well. However, we also calculated $^{17}W_c/^{89}W_c$ following the Millis-Monien-Pines model, including the form factor [Eq. (11)] proposed by Zha, as well as the incommensurability. The result is plotted in Fig. 12 and shows clearly, that this

ansatz fails. While the nearly constant value of $^{17}W_c/^{89}W_c$ at temperatures above T^\dagger agrees with the calculation, the pronounced upturn of the ratio below T^\dagger and its saturation around 100 K are not reproduced by the model. That the model fails in this case can be seen quite easily. Since one assumes the single-spin fluid model, there is just one $\chi''(\mathbf{q}, \omega)$ relevant for the spin-lattice relaxation rate [Eq. (9)]. The normalized form factors [Eqs. (11) and (12)] for O(2,3) and Y are almost the same, so that also the T_1 's will exhibit almost the same temperature behavior resulting in a very weak temperature dependence of $^{17}W_c/^{89}W_c$.

An upturn of the $^{17}W_c/^{89}W_c$ in $\text{YBa}_2\text{Cu}_4\text{O}_8$ has also been observed by Kambe *et al.*¹⁵ although their data differ from ours. On the other hand, it is puzzling that the $^{17}W_c/^{89}W_c$ ratio in *underdoped* $\text{YBa}_2\text{Cu}_3\text{O}_{6.63}$ and *overdoped* $\text{YBa}_2\text{Cu}_3\text{O}_7$ exhibits only a weak temperature dependence¹⁷ (see Fig. 12).

Tagikawa *et al.*¹⁷ and Kambe *et al.*¹⁵ attributed the temperature dependence of $^{17}W_c/^{89}W_c$ to the growing, with decreasing temperature, of interplane antiferromagnetic correlations. Indeed, the presence of very strong antiferromagnetic correlations between adjacent planes in underdoped Y-Ba-Cu-O compounds has been shown by a number of experiments, for instance by neutron-scattering⁴³ and SEDOR experiments.⁴⁵ However, it is questionable whether the growth of the interplane correlations alone suffices to explain the extraordinary increase of $^{17}W_c/^{89}W_c$ we and Kambe *et al.* observe in $\text{YBa}_2\text{Cu}_4\text{O}_8$ below 180 K.

We therefore, as a supplement to the correlation growth effect, propose the presence of an additional relaxation mechanism which can provide a coherent description of the temperature dependence of both $^{17}(W_{\parallel}/W_{c,\perp})$ and $^{17}W_c/^{89}W_c$. As shown in Sec. V B, there are enhanced charge fluctuations in the chain and the plane at temperatures below T^\dagger . These fluctuations open an additional relaxation channel which is of *quadrupolar* origin. This would easily explain the temperature dependence of $^{17}W_c/^{89}W_c$ (see Fig. 12) since only $^{17}W_c$ of O(2,3) is enhanced, while yttrium, because of its spin 1/2, cannot couple to the charge fluctuations. Of course, the upturn of $^{17}W_c/^{89}W_c$ is a large effect compared to the relatively small anomalies occurring at T^\dagger and it could very well be that the $^{17}W_c/^{89}W_c$ upturn is caused by a different mechanism. Nevertheless, the fact that all these effects occur around the same temperature is very tempting for suggesting a *common* mechanism.

The relative magnitude of the quadrupolar contribution to the total relaxation rate, $^{17}W_c$, of O(2,3) can be calculated as follows. We assume that the magnetic and quadrupolar contributions are almost independent of each other and that both yttrium and O(2,3) couple to the same spin degree of freedom, described by $\chi''(\mathbf{q}, \omega)$. Since the form factors for these two isotopes, within the Mila-Rice Hamiltonian, are very similar [Eqs. (11) and (12)], T_1 as given by Eq. (9) should exhibit almost the same temperature dependence for Y and O(2,3). This then allows one to separate the magnetic and the quadrupolar contribution to $^{17}W_c$. We obtain

$$^{17}W_c^{\text{quad}} \approx \left[\frac{^{17}W_c}{^{89}W_c} - \left(\frac{^{17}W_c}{^{89}W_c} \right)_{300\text{K}} \right] ^{89}W_c \quad (17)$$

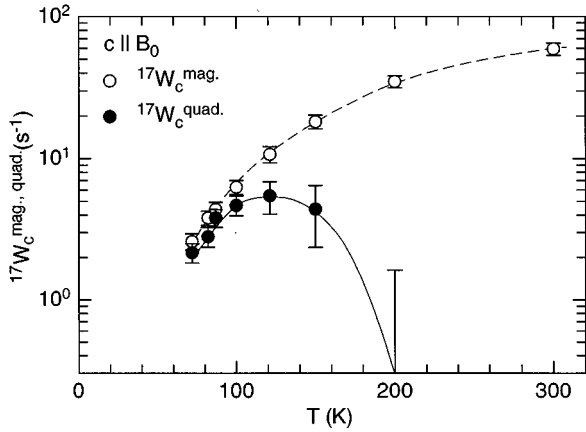


FIG. 13. $^{17}W_c^{\text{quad}}$ and $^{17}W_c^{\text{mag}}$ vs temperature of O(2,3). The lines serve as a guide to the eyes.

and $^{17}W_c^{\text{mag}} = ^{17}W_c - ^{17}W_c^{\text{quad}}$. Below 100 K, the two contributions are of the same order of magnitude (see Fig. 13). In view of the temperature dependence of $^{17}(W_{\parallel}/W_c)$, it follows that the quadrupolar fluctuations have to be the strongest along the Cu-O bond.

Accepting this analysis, one immediately wonders why the quadrupolar contribution is not detected at the plane Cu site. At this site, the spin-lattice relaxation rate is dominated by the strong antiferromagnetic fluctuations, that means $\chi''(\mathbf{Q}_{\text{AF}}) \gg \chi''(\mathbf{0})$, while these fluctuations are filtered at the oxygen and yttrium sites. Therefore, the relatively small quadrupolar contribution to W_{α} of Cu(2) is difficult to detect.

A final question in this context is whether, in the presence of a quadrupolar contribution, the procedure to determine the T_1 values has been correct. We have fitted the magnetization recovery data by formulas which were derived for purely magnetic fluctuations.⁴⁶

$$M(t) = M(\infty) \left[1 - A \sum_i c_i \exp\left(-\frac{t\lambda_i}{2T_1}\right) \right], \quad (18)$$

where A and c_i are given by the initial conditions and the λ_i 's are the eigenvalues of the master equation. As we have shown elsewhere,⁴⁷ even for strong quadrupolar contributions, i.e., $W^{\text{quad}} \approx W^{\text{mag}}$, and our initial conditions, the coefficients c_i as well as the eigenvalues λ_i are only marginally changed. Therefore, the extracted T_1 values are correct within the error bars.

D. A charge-density-wave model

We finally speculate on the possible mechanism for the charge redistribution and the enhancement of the charge fluctuations below T^{\dagger} . Recently, Eremin *et al.*⁴⁸ have argued that the so-called ‘‘spin-gap’’ phenomenon in $\text{YBa}_2\text{Cu}_4\text{O}_8$ is caused by a transition due to a charge-density wave (CDW). The notion ‘‘spin-gap effect’’ refers to the opening of a pseudogap in the electron-spin excitation spectrum at a temperature $T_S \approx 150$ K which lies above T_c . This effect explains the strong temperature dependence of the normal-state susceptibility in $\text{YBa}_2\text{Cu}_4\text{O}_8$. The proximity of T^{\dagger} and T_S has been a trigger for these investigations.

It is known that a two-dimensional Fermi-like liquid is unstable with respect to a CDW transition if the chemical potential is located near the energy where the density of states exhibits the Van Hove saddle singularity peak. Starting from the t - J model and including electron-phonon interaction, Eremin *et al.* derived the gap equation for a charge-density wave in the CuO plane, using the singlet correlated band in the normal state. From their analysis, the authors could explain, e.g., the strong temperature dependence of $^{65}K_{ab}$ of Cu(2) as well as the opening of the spin gap.

Therefore, it is very tempting to explain the enhanced charge fluctuations we observe below T^{\dagger} by means of a transition to a CDW. Our results have shown that enhanced charge fluctuations also occur in the chain and our analysis strongly suggests a charge transfer from the chain to the plane. Since the origin of the transfer seems to be located in the plane rather than in the chain and, on the other hand, the CDW also seems to occur in the plane, it looks as if the charge transfer is triggered by the CDW of the plane.

VI. SUMMARY

We have performed an NMR and NQR study, respectively, of the Cu, O, and Y isotopes in the normal state of the high-temperature superconductor $\text{YBa}_2\text{Cu}_4\text{O}_8$. From measurements of the temperature dependence and, in some cases, the anisotropy of various NMR/NQR quantities such as relaxation times, Knight shifts, NQR frequencies, and linewidths, we have obtained the two following major results:

(i) The magnetic shifts scale among each other which implies that the hyperfine interaction in the plane as well as in the chain is determined by one spin degree of freedom, i.e., the Cu 3d holes and the doped holes, which mainly go into O 2p states, are described by only *one* susceptibility. However, the susceptibility for the plane is different from that of the chain.

(ii) Around $T^{\dagger} = 180$ K, we detected ‘‘anomalies’’ in the temperature behavior of several NMR/NQR quantities. We interpret the anomalies as the fingerprint of an electronic crossover, rather than a structural phase transition, occurring in both the planes and chains once the temperature is lowered below T^{\dagger} . The crossover reveals itself by enhanced charge fluctuations in planes and chains accompanied by a charge (hole) transfer from chain to plane.

A possible mechanism of the crossover could be a charge-density-wave instability. The occurrence of such instabilities in the normal state of cuprate superconductors has recently been discussed by Eremin *et al.*⁴⁸ This model is able to explain some of the observed features, if one assumes that T^{\dagger} is the temperature below which the charge-density wave is formed.

ACKNOWLEDGMENTS

It is a pleasure to thank A. Lombardi, R. Markendorf, I. Eremin, and M. Eremin for many illuminating discussions. Partial support of this work by the Swiss National Science Foundation is gratefully acknowledged.

- ¹A. Abragam, *The Principles of Nuclear Magnetism* (Clarendon, Oxford, 1961).
- ²T. Moriya, J. Phys. Soc. Jpn. **18**, 516 (1963).
- ³K. Yoshida and T. Moriya, J. Phys. Soc. Jpn. **11**, 33 (1956).
- ⁴F. Mila and T.M. Rice, Physica C **157**, 561 (1989).
- ⁵Y. Zha, V. Barzykin, and D. Pines, Phys. Rev. B **54**, 7561 (1996).
- ⁶A.J. Millis and H. Monien, Phys. Rev. B **45**, 3059 (1992).
- ⁷J. Karpinski, E. Kaldis, E. Jilek, S. Rusiecki, and B. Bucher, Nature (London) **336**, 660 (1988).
- ⁸I. Mangelschots, M. Mali, J. Roos, D. Brinkmann, S. Rusiecki, J. Karpinski, and E. Kaldis, Physica C **194**, 277 (1992).
- ⁹M. Bankay, M. Mali, J. Roos, and D. Brinkmann, Phys. Rev. B **50**, 6416 (1994).
- ¹⁰M. Mali, I. Mangelschots, H. Zimmermann, and D. Brinkmann, Physica C **175**, 581 (1991).
- ¹¹H. Zimmermann, Ph.D. thesis, Universität Zürich, 1991.
- ¹²H.Y. Carr and E.M. Purcell, Phys. Rev. **94**, 630 (1954); S. Meiboom and D. Gill, Rev. Sci. Instrum. **29**, 6881 (1958).
- ¹³J.A. Martindale, S.E. Barrett, D.J. Durand, E. O'Hara, C.P. Slichter, W.C. Lee, and D.M. Ginsberg, Phys. Rev. B **50**, 13 645 (1994).
- ¹⁴J.A. Martindale, P.C. Hammel, W.L. Hults, and J.L. Smith (unpublished).
- ¹⁵S. Kambe, T. Machi, I. Tomeno, H. Yasuoka, A. Hayashi, and Y. Ueda, J. Phys. Soc. Jpn. **63**, 3481 (1994).
- ¹⁶R. Dupree, Z.P. Han, D. McK. Paul, T.G.N. Babu, and C. Greaves, Physica C **179**, 311 (1991).
- ¹⁷M. Takigawa, W.L. Hults, and J.L. Smith, Phys. Rev. Lett. **71**, 2650 (1993).
- ¹⁸H. Alloul, A. Mahajan, H. Casalta, and O. Klein, Phys. Rev. Lett. **70**, 1171 (1993).
- ¹⁹I. Mangelschots, M. Mali, J. Roos, R. Stern, M. Bankay, A. Lombardi, and D. Brinkmann, Proceedings of the International School of Solid State Physics: *3rd Workshop on Phase Separation in Superconductors* (World Scientific, Singapore, 1993), p. 262.
- ²⁰G. Zheng, Y. Kitaoka, K. Asayama, Y. Kodama, and Y. Yamada, Physica C **193**, 154 (1992).
- ²¹I. Tomeno, T. Machi, K. Tai, N. Koshizuka, S. Kambe, A. Hayashi, Y. Ueda, and H. Yasuoka, Phys. Rev. B **49**, 15 327 (1994).
- ²²H. Zimmermann, M. Mali, D. Brinkmann, J. Karpinski, E. Kaldis, and S. Rusiecki, Physica C **159**, 681 (1989).
- ²³F.C. Zhang and T.M. Rice, Phys. Rev. B **37**, 3759 (1988).
- ²⁴A. Lombardi, M. Mali, J. Roos, and D. Brinkmann, Physica C **267**, 261 (1996).
- ²⁵O.V. Alexandrov, M. Francois, T. Graf, and K. Yvon, Physica C **170**, 56 (1990).
- ²⁶H.A. Ludwig, W.H. Fietz, M.R. Dietrich, and H. Wuhl, Physica C **167**, 335 (1990).
- ²⁷H. Schwer (private communication).
- ²⁸In contrast to Ca doped $Y_{1-x}Ba_{2-y}Ca_{x+y}Cu_4O_8$, where NMR/NQR studies (Ref. 49) and x ray studies (Ref. 50) showed a structural phase transition at 150 K for Ca doping $\geq 2\%$.
- ²⁹Wu Ting, K. Fossheim, T. Wada, Y. Yaegashi, H. Yamauchi, and S. Tanaka, Phys. Rev. B **47**, 12 197 (1993).
- ³⁰T.R. Sendyka, W. Dmowski, T. Egami, N. Seiji, H. Yamauchi, and S. Tanaka, Phys. Rev. B **51**, 6747 (1995).
- ³¹J.-S. Zhou, J.B. Goodenough, B. Dabrowski, and K. Rogacki, Phys. Rev. Lett. **77**, 4253 (1996).
- ³²S.E. Barrett, D.J. Durand, C.H. Pennington, C.P. Slichter, T.A. Friedmann, J.P. Rice, and D.M. Ginsberg, Phys. Rev. B **41**, 6283 (1990).
- ³³R.E. Walstedt, W.W. Warren, Jr., R.F. Bell, R.J. Cava, G.P. Espinosa, L.F. Schneemeyer, and J.V. Waszczak, Phys. Rev. B **41**, 9574 (1990).
- ³⁴S. Ohsugi, Y. Kitaoka, K. Ishida, G.-q. Zheng, and K. Asayama, J. Phys. Soc. Jpn. **63**, 700 (1994).
- ³⁵Since the field H_{c2} is rather anisotropic, the charge-carrier density for $c\parallel B_0$ and $c\perp B_0$ differ in the vicinity of T_c . That is why we measured, at this temperature, $^{17}(W_{\parallel}/W_{\perp})$ rather than $^{17}(W_{\parallel}/W_c)$. However, Martindale *et al.* (Ref. 14) showed that $^{17}(W_{\perp}/W_c)$ is temperature independent above T_c , so that one just has to rescale this data point by $(C_{\parallel}^2 + C_c^2)/(C_{\parallel}^2 + C_{\perp}^2)$ which is approximately 1.08 for $YBa_2Cu_4O_8$.
- ³⁶F. Barriquand, P. Odier, and D. Jérôme, Physica C **177**, 230 (1991).
- ³⁷M. Horvatić, C. Berthier, Y. Berthier, P. Ségransan, P. Butaud, W.G. Clark, J.A. Gillet, and J.Y. Henry, Phys. Rev. B **48**, 13 848 (1993).
- ³⁸If one would assume a change of the hyperfine coupling constants C_{α} below T^{\dagger} , this would also imply a change in the hyperfine couplings D_{α} of yttrium, since yttrium couples at O(2,3) (Refs. 51 and 52). Since $^{89}(W_{\parallel}/W_c)$ is temperature independent, this cannot be the case.
- ³⁹J. Rossat-Mignod, L. R. Regnault, C. Vettier, P. Burlet, J.Y. Henry, and G. Lapertot, Physica B **169**, 58 (1991); J. Rossat-Mignod, L.P. Regnault, C. Vettier, P. Bourges, P. Burlet, J. Bossy, J.Y. Henry, and G. Lapertot, *ibid.* **180-181**, 383 (1992); P. Bourges, L.P. Regnault, J.Y. Henry, C. Vettier, Y. Sidis, and P. Burlet, *ibid.* **215**, 30 (1995).
- ⁴⁰H.A. Mook, M. Yethiraj, G. Aeppli, T.E. Mason, and T. Armstrong, Phys. Rev. Lett. **70**, 3490 (1993).
- ⁴¹P. Dai, H.A. Mook, G. Aeppli, F. Doğan, K. Salama, and D. Lee (unpublished).
- ⁴²H.F. Fong, B. Keimer, P.W. Anderson, D. Reznik, F. Doğan, and I.A. Aksay, Phys. Rev. Lett. **75**, 316 (1995).
- ⁴³J.M. Tranquada, P.M. Gehring, G. Shirane, S. Shamoto, and M. Sato, Phys. Rev. B **46**, 5561 (1993).
- ⁴⁴B.J. Sternlieb, G. Shirane, J.M. Tranquada, M. Sato, and S. Shamoto, Phys. Rev. B **47**, 5320 (1993).
- ⁴⁵R. Stern, M. Mali, J. Roos, and D. Brinkmann, Phys. Rev. B **52**, R15 734 (1995).
- ⁴⁶E.R. Andrew and D.P. Tunstall, Proc. Phys. Soc. London **78**, 1 (1961).
- ⁴⁷A. Suter *et al.* (unpublished).
- ⁴⁸I. Eremin, M. Eremin, S. Varlamov, D. Brinkmann, M. Mali, and J. Roos (unpublished).
- ⁴⁹M. Mali, J. Roos, and D. Brinkmann, Phys. Rev. B **53**, 3550 (1996).
- ⁵⁰H. Schwer, J. Karpinski, and E. Kaldis, Physica C **235-240**, 801 (1994).
- ⁵¹F.J. Adrian, Phys. Rev. Lett. **61**, 2148 (1988).
- ⁵²H. Alloul, T. Ohno, and P. Mendels, Phys. Rev. Lett. **63**, 1700 (1989).